Solid-State Chemistry of Ambroxol Theophylline-7-Acetate

ANASTASIA FOPPOLI,[1] LUCIA ZEMA,[1] ANDREA GAZZANIGA,[1] MINO R. CAIRA,[2]
LUIGI R. NASSIMBENI,[2] EVAN BORKUM,[2] RUGGERO BETTINI,[3] FERDINANDO GIORDANO[3]

[1]Istituto di Chimica Farmaceutica e Tossicologica ''Pietro Pratesi'', University of Milano, 20131 Milano, Italy

[2]Department of Chemistry, University of Cape Town, 7701 Rondebosch, Cape Town, South Africa

[3]Dipartimento Farmaceutico, University of Parma, 43100 Parma, Italy

Received 31 August 2006; revised 13 November 2006; accepted 14 November 2006

Published online in Wiley InterScience (www.interscience.wiley.com). DOI 10.1002/jps.20951

ABSTRACT: Ambroxol theophylline-7-acetate (ACE) is the salt obtained by reaction of equimolar amounts of ambroxol (AMB), a drug showing mucolytic and expectorant properties, and theophylline-7-acetic acid (TAA), a xanthine derivative with specific bronchodilator activity. ACE is used for the treatment of bronchial and pulmonary diseases (bronchitis, asthma, emphysema, chronic obstructive disease). Recrystallization experiments of ACE resulted in the isolation of two polymorphs (monotropically related) and four solvated forms. X-ray diffractometry, DSC, TGA, and HSM techniques were used to investigate the forms that are obtained by thermal desolvation of the solvates. The phase diagram of the TAA–AMB binary system was constructed by performing thermal analyses on mixtures of TAA–AMB and of each component plus the interaction compound (TAA–ACE and ACE–AMB). The Schroeder–Van Laar equation proved to be a very useful tool for checking the consistency between the experimental data and the theoretical model related to the general system, showing complete miscibility in the liquid phase and complete immiscibility in the solid phase.
 J Pharm Sci 96:1139–1146, 2007
Keywords: solid state; polymorphism; pseudopolymorphism; X-ray powder diffractometry; thermal analysis

INTRODUCTION

The ability of an element or compound to exist in multiple crystalline states with different structural arrangements is termed polymorphism. When solvent molecules (water, in the great majority of cases with pharmaceutical relevance) are stoichiometrically entrapped in the crystal structure of the compound, solvates are generated.[1]

Solid-state properties, for example, melting point, density, solubility, morphology, flowability, compactability, can differ dramatically from one polymorph to another. The same holds, of course, for unsolvated/solvated forms, for solvates each containing a different number of solvent molecules, and, obviously, for polymorphs of the same solvate. Polymorphic transitions and solvation/desolvation phenomena can occur unwittingly, for example, during unit processes such as grinding, granulation, or drying. Moreover, a thermodynamically metastable yet kinetically stable crystal form could convert to a thermodynamically more stable crystal form on storage. As a consequence, the manufacturing process and the biopharmaceutical properties of a pharmaceutical dosage form can be severely compromised, when new or unexpected crystal phases of the active ingredient or even of the excipients are involved. This leads to the need for a thorough preliminary characterization of the solid-state properties of each component within the pharmaceutical formulation,

Correspondence to: Ferdinando Giordano (Telephone: 0039 0521 905079; Fax: 0039 0521 905006;
E-mail: ferdinando.giordano@unipr.it)

Journal of Pharmaceutical Sciences, Vol. 96, 1139–1146 (2007)

aiming to deal always with the same polymorphic (or solvate) form.[2]

Ambroxol, (trans-((amino-2-dibromo-3,5-benzyl) amino)-4-cyclohexanol CAS No. 18683-91-5, AMB, Fig. 1a), generally used as the hydrochloride salt, shows remarkable mucolytic and expectorant properties and is the active pharmaceutical ingredient (API) of several marketed drug products (Mucosolvan® Boehringer Ingelheim, Fluibron® Chiesi, Italy). Recently, AMB has also been proposed for the treatment of pulmonary alveolar proteinosis[3] and for *sicca keratoconjunctivitis* associated with Sjögren syndrome.[4]

Theophylline-7-acetic acid (1,2,3,6-tetrahydro-1,3-dimethyl-2,6-dioxopurine-7-acetic acid, TAA, Fig. 1b) is a derivative of theophylline, a xanthine extensively used for its diuretic, cardiac stimulant, and smooth muscle relaxant pharmacological effects. With respect to the parent compound, TAA has a similar but more specific bronchodilator activity.[5] The carboxylic function has been exploited to prepare esters[6] and various salts with pharmacologically active organic bases (e.g., mepyramine,[7] N,N-diethylaminoethanol,[8] xylocaine,[9] procainamide,[10] drotaverine,[11,12] and AMB[13]). Among these salts, Ambroxol theophylline-7-acetate (acebrophylline, CAS No. 96989-76-3, ACE, Fig. 1c) is the API of marketed drug products (Broncomnes® Bracco, Surfolase® Pharmacia, Ambromucil® Malesci, Italy). It can be easily prepared by the reaction of equimolar amounts of TAA and AMB in an aprotic solvent and subsequent precipitation. It shows the expectorant and secretolytic activity of AMB and the bronchodilator activity of the theophylline derivative, making it especially valuable for the treatment of bronchitis, bronchial asthma, emphysema, and chronic obstructive pulmonary disease.[14,15]

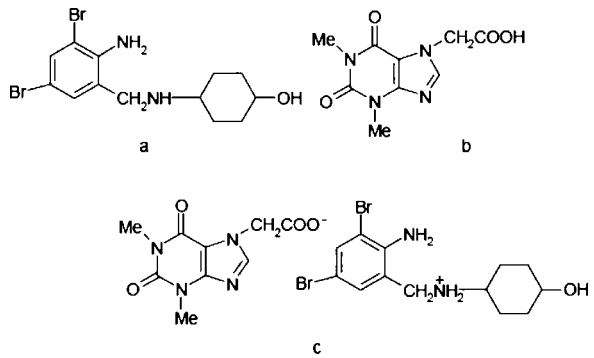

Figure 1. Structural formulas of (a) AMB, (b) TAA, and (c) ACE.

Regarding the solid-state chemistry of AMB, TAA, and ACE, thus far the polymorphism of both AMB and TAA has been investigated,[16,17] whereas concerning the title compound ACE, only the crystal structures of ambroxol theophylline-7-acetate monohydrate[18] and of a nickel(II) compound containing uncoordinated theophylline-7-acetate ion[19] have been reported.

The present paper aims to give a comprehensive picture of the solid-state properties of ACE. Polymorphism and solvatomorphism of this compound were investigated by analytical techniques such as thermal analysis (DSC, TGA, HSM), and X-ray powder diffractometry. Thermal data were also used to trace the phase diagram of the TAA–AMB binary system.

EXPERIMENTAL

Materials

AMB hydrochloride was purchased from ICN Biomedicals Inc. (Aurora, OH) and TAA was a generous gift of Erregierre SpA (San Paolo d'Argon BG, I); both were used as received. Certificates of analysis reflecting the purity (>99.5%) of the starting materials were available from the suppliers. AMB (free base) was obtained by dissolving AMB hydrochloride in water (13 g/L at 60°C) and by adding dropwise, under stirring, aqueous NaOH to a pH value of ~9.5. The resulting suspension was then allowed to stand overnight at 4°C, filtered under vacuum, washed repeatedly with water, and air-dried at ambient temperature.

ACE was prepared by dissolving equimolar amounts of AMB and TAA in absolute ethanol and evaporating the solvent by gentle heating under vacuum.

Physico-chemical data of both AMB and ACE (elemental analyses for CHN, FTIR as KBr disk and NMR spectra in D_2O) were consistent with their structural formulas. The yield for the crystallization of AMB and ACE was >95% in all cases.

Binary mixtures were prepared by gentle mixing of suitably calculated and accurately weighed amounts of components in a mortar with a spatula without exerting undue pressure.

All solvents used were of analytical purity grade, and were dried before use over 3 Å molecular sieves.

 DOI 10.1002/jps

Methods and Apparatus

Recrystallization Procedures

Recrystallizations were conducted by dissolving approximately 250 mg samples of ACE in the minimum amount of solvent (water, methanol, ethanol, 1- and 2-propanol, acetone, 1,4-dioxane) or solvent mixture, at temperatures of a few degrees below the boiling point of the solvent. The saturated solution was then filtered while hot (0.45 μm nylon microfilter) and left to recrystallize by spontaneous cooling and evaporation at room temperature. Recrystallized products were obtained in a period of 1–7 days (2 days on average), isolated by suction filtration and air-dried at ambient temperature prior to solid-state analyses.

Thermal Analysis

Differential Scanning Calorimetry (DSC) and Thermogravimetric Analysis (TGA)

Data were collected by means of TA instruments (New Castle, DE), namely a DSC2010 calorimeter and a TG2050 thermobalance, between ambient temperature and approximately 250°C, under nitrogen purging of 70 mL min^{-1}. DSC runs were performed on 2–3 mg samples in nonhermetically sealed aluminum pans at a scanning rate of 10 K min^{-1}; TGA was performed on 15–20 mg samples at 10 K min^{-1}. As for binary mixtures, only first heating runs were considered since evaporation/decomposition of the low melting components (AMB and ACE) occurred during DSC scans above 200°C.

All the reported values are the averages of at least six determinations.

Hot Stage Microscopy (HSM)

A hot stage apparatus (HSF 91, Linkam Scientific Instruments, Tadworth, UK) equipped with a microscope (Labophot II polarizing microscope, Nikon, Tokyo, J) was used as supplementary source of information. A 3CCD color video camera module (XC-003P Sony, Tokyo, J), supported by Image-Pro® Plus 4.0 software, allowed the recording of images during temperature scans.

Powder samples suspended in silicone oil were observed under the hot stage microscope. The evolution of bubbles on heating can be unequivocally attributed to solvent loss, since no mass change was observed in the same temperature range for anhydrous ACE, thus suggesting that the compound is stable with respect to decomposition/sublimation processes.

Powder X-Ray Diffraction (PXRD)

A Philips PW1050/25 diffractometer (Philips Analytical Inc., Natick, MA) using Cu-K_α radiation ($\lambda = 1.5418$ Å) generated with 40 kV and 20 mA was employed. The system was calibrated with a silicon standard which yielded peak positions of $28.45 \pm 0.01°2\theta$ before and after each scan. All samples were packed in the same aluminum sample holder for reproducibility of conditions, taking care to also minimize preferred orientation effects. Full PXRD traces (scan speed 1.0° 2θ min^{-1}, step size 0.1° 2θ, 2θ-range 5–35°) were recorded.

RESULTS AND DISCUSSION

Isolation and Characterization of Crystal Phases

One anhydrous and four solvated forms of ACE were isolated by recrystallization trials. A second anhydrous form was obtained by thermal desolvation of the hydrate. This form could not be isolated by recrystallization from solvent. Tab. 1 collects the information relevant to the preparation of ACE solid phases.

Table 1. Crystal Forms of ACE and Relevant Methods of Preparation

Crystal Form	Method of Preparation
ACE I	Crystallization from acetone, 1- and 2-propanol
ACE · H_2O	Crystallization from water and water/alcohol mixtures (1:1, v:v)
ACE · 1,4-dioxane	Crystallization from 1,4-dioxane
ACE · nMeOH*	Crystallization from methanol
ACE · nEtOH*	Crystallization from ethanol
ACE II	By heating ACE · $H_2O > 100$°C

*The stoichiometry could not be assessed, see below.

PXRD patterns of ACE crystal forms at room temperature are presented in Figure 2.

Distinctive peaks are detectable for all forms but the methanol and ethanol solvates show a close correspondence of peaks, suggesting the isostructurality of these phases. This implies that the three-dimensional arrangement of ACE is a common structural motif in both the alcoholates and that the included ethanol/methanol molecules occupy common crystallographic sites.

Both the alcoholates tend to convert to ACE · H_2O when exposed to ambient conditions (over a timescale of 1 month).

DSC and TGA traces and the relevant thermal data (peak T_{onset} and ΔH) are reported in Figure 3 and Tab. 2, respectively.

Two ACE anhydrous solid phases have been obtained, with melting points (T_{max}) at 219 and 215°C (Fig. 3a and b). According to the generally accepted nomenclature for polymorphs, the high melting polymorph was labeled Form I and consequently the other Form II. No mass change is observed up to the melting event; however a remarkable weight loss due to drug decomposition is observed above the melting temperature. According to Burger and Ramberger's heat of fusion rule,[20] Form II is in a monotropic relationship with Form I and represents the metastable polymorph. This is further demonstrated by the conversion of Form II to Form I when suspended in acetone.

Concerning the solvates from water and 1,4-dioxane (Fig. 3c and d), the desolvation process is clearly reflected by a distinct endotherm and a single step mass loss in the TGA trace, closely corresponding to the calculated w/w percentage loss for a 1:1 stoichiometry (calculated weight change = 2.84% and 12.5%, experimental weight change = 2.79% and 12.18% for the water and 1,4-dioxane solvate, respectively). After solvent removal, different anhydrous phases can be recovered and identified unambiguously by comparison with traces shown in Figure 2: Form I is obtained from the 1,4-dioxane solvate, as evidenced by the subsequent melting endotherm at 219°C, while ACE · H_2O dehydrates to Form II which readily converts (<1 h) into the original monohydrate by exposure to ambient temperature and humidity.

ACE · nMeOH and ACE · nEtOH present a similar complex thermal behavior. The DSC traces (Fig. 3e and f) display a broad and almost flat endotherm within the room temperature–100°C range, corresponding to desolvation. Due to the flat nature of the endotherm, it was virtually impossible to determine the onset temperature. Also the percentage mass loss could not be assessed with accuracy due to the high variability of desolvation between samples. This variability can be attributed to factors such as particle size and exposed surface area, although no specific quantitative assessment of these factors was performed.

Subsequent to desolvation, another endotherm was observed at approximately 160°C, immediately followed by an exothermic event. At this

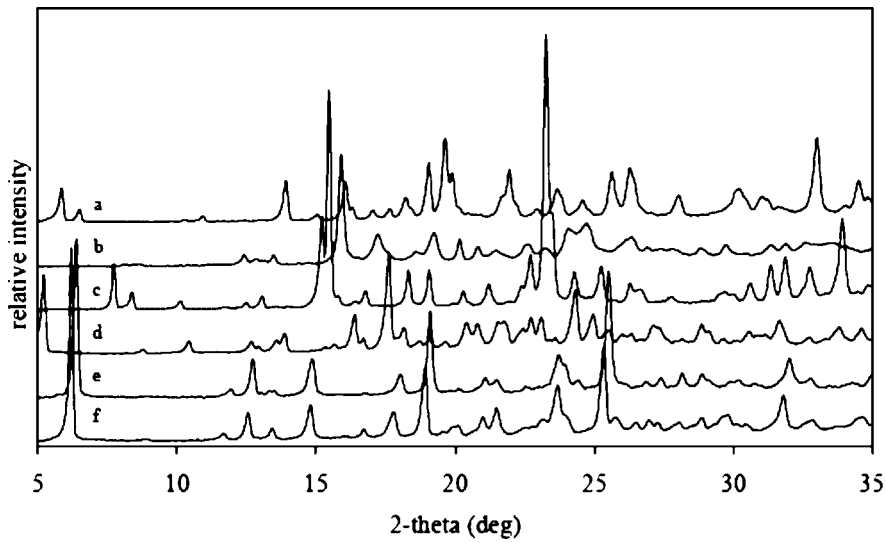

Figure 2. PXRD patterns of ACE crystal phases: (a) Form I, (b) Form II, (c) ACE · H_2O, (d) ACE · 1,4-dioxane, (e) ACE · nMeOH, and (f) ACE · nEtOH.

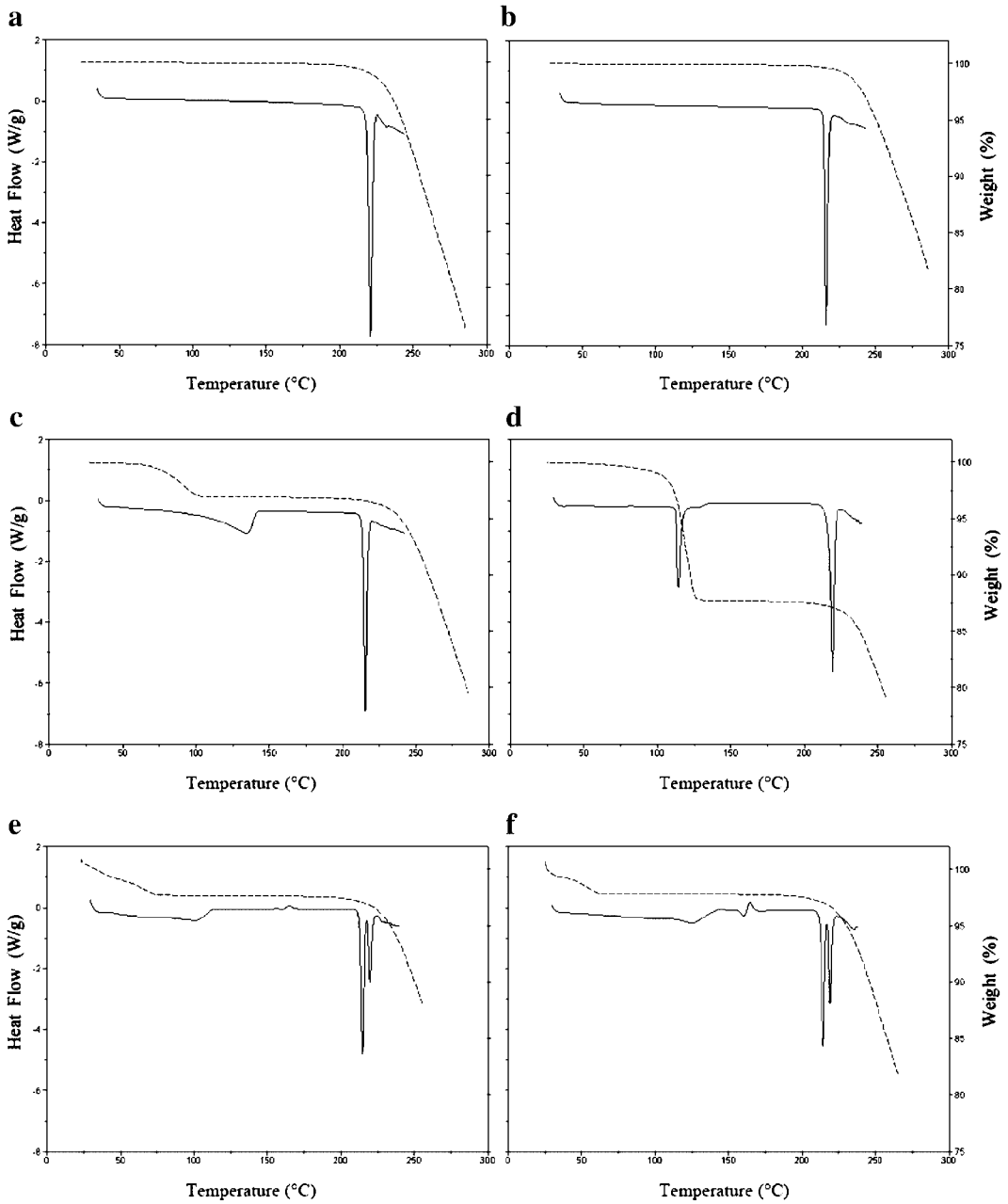

Figure 3. DSC (—) and TGA (---) traces of ACE crystal phases: (a) Form I, (b) Form II, (c) ACE · H_2O, (d) ACE · 1,4-dioxane, (e) ACE · nMeOH, and (f) ACE · nEtOH.

temperature, TGA did not exhibit any mass loss. By means of HSM it was observed that, between 160 and 170°C, the desolvated crystals undergo a major physical change, involving the growth of a new solid phase, with progressive variation in the transparency of the crystals. The endo/exo event in the DSC trace can be likely ascribed to a polymorphic transition, involving the melting of the desolvation product and simultaneous recrystallization to a mixture of Forms I and II. Therefore, one interpretation of these results is that a third polymorphic form of ACE, tentatively labeled Form III, exists. Unfortunately, attempts to isolate Form III by heating the alcoholates above the desolvation temperature followed by cooling to ambient conditions were unsuccessful.

Table 2. DSC Data for ACE Solid Phases (Mean Values, $n = 6$, Standard Deviation In Parentheses)

	Desolvation		Fusion		Recrystallization		Final Fusion	
Crystal Form	T_{onset} (°C)	ΔH (Jg^{-1})	T_{onset} (°C)	ΔH (Jg^{-1})	T_{onset} (°C)	ΔH (Jg^{-1})	T_{onset} (°C)	ΔH (Jg^{-1})
Form I	—	—	—	—	—	—	218.4 (0.7)	143.0 (8.6)
Form II	—	—	—	—	—	—	214.6 (0.7)	101.5 (3.0)
ACE · H_2O	115.4 (9.1)	112.5 (14.6)	—	—	—	—	214.5 (0.8)	100.4 (1.7)
ACE · 1,4-dioxane	111.9 (2.6)	65.6 (2.6)	—	—	—	—	218.5 (0.3)	108.5 (2.7)
ACE · nMeOH	nq*	nq*	157.1 (1.0)	4.2 (2.7)	160.5 (10.1)	−9.3 (1.5)	212.7 (0.5) 217.8 (0.4)	nd**
ACE · nEtOH	nq*	nq*	157.7 (0.6)	4.3 (2.3)	164.3 (5.1)	−7.8 (2.4)	212.5 (0.7) 217.7 (0.5)	nd**

*Not quantifiable.
**Peaks not separated.

Phase Diagram of the TAA–AMB Binary System

The TAA–AMB binary system was investigated by performing thermal analyses (DSC, TGA, and HSM) on mixtures of TAA–AMB and of each component plus the interaction compound (TAA–ACE and ACE–AMB).

Figure 4 reports the DSC and TGA traces of pure components AMB and TAA and of the interaction compound ACE. In Figure 5 the thermal behaviors of mixtures with mole fractions of AMB (x_{AMB}) = 0.1, 0.3, and 0.8 are shown.

All binaries show the solid–liquid transition of the low melting component AMB (~95°C) and the recrystallization exotherm of the interaction compound within the 130–160°C temperature range, as confirmed by HSM. The original binary system composition at this point has changed from TAA–AMB to ACE (for $x_{AMB} = 0.5$), or to ACE plus the excess component (TAA or AMB). The possibility of a metastable eutectic fusion was excluded by evaluating the fusion enthalpies around 95°C which were, for all compositions tested, proportional to the AMB content of each mixture (for both systems, TAA–AMB and ACE–AMB). This leads to the obvious conclusion that neither the free acid, TAA, nor the salt, ACE, are appreciably soluble in liquid AMB below 160°C.

All mixtures with $x_{AMB} < 0.5$ show two distinct endotherms above 160°C. The first, occurring at fixed temperature (212°C), corresponds to the eutectic fusion within the TAA–ACE binary system (see Fig. 6). The second is a broad endotherm representing the progressive solubilization of the excess component (TAA or ACE) with respect to the eutectic composition ($x_{AMB} = 0.44$). For mixtures containing $x_{AMB} > 0.5$, in addition to

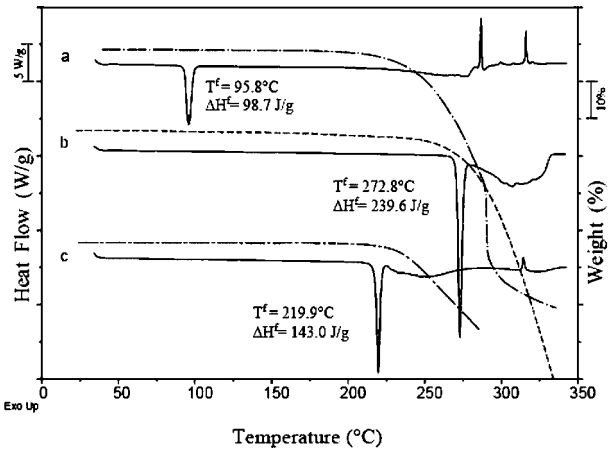

Figure 4. DSC and TGA traces of pure (a) AMB, (b) TAA, and (c) ACE.

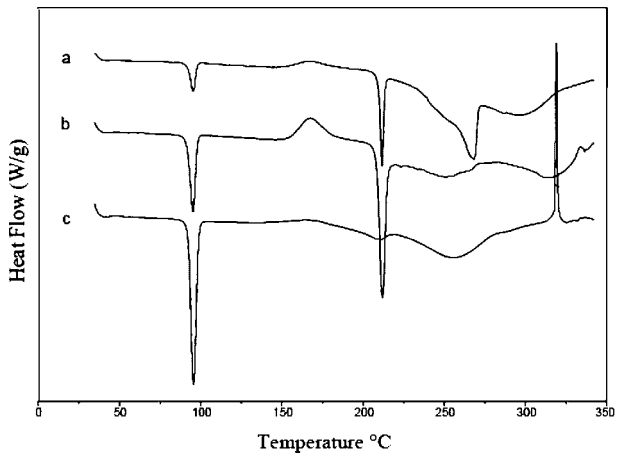

Figure 5. Thermal behavior of TAA–AMB mixtures (curve a: $x_{AMB} = 0.1$; curve b: $x_{AMB} = 0.3$; curve c: $x_{AMB} = 0.8$).

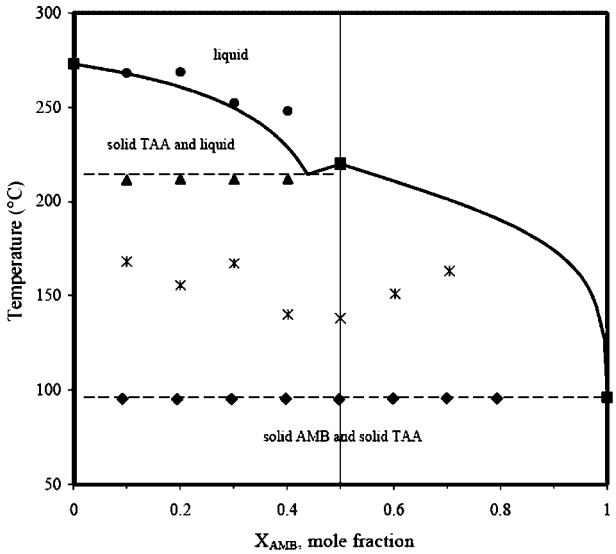

Figure 6. Phase diagram of the TAA–AMB binary system. Solid lines represent the calculated liquidus curves; experimental points: (◆) melting of AMB, (✳) recrystallization of the interaction compound, (▲) eutectic fusion, (●) final fusion, (■) melting of pure solid phases (TAA, ACE, and AMB).

thermal events presented by all binaries, the experimental thermal behavior is increasingly different from the theoretical one. As anticipated, the concomitant evaporation/decomposition of AMB and ACE at high temperatures (above ~200°C) reasonably accounts for this deviation (see Fig. 4, traces a and c).

Thermal data from DSC runs were used to calculate the theoretical binary phase diagrams of the TAA–AMB, TAA–ACE, and ACE–AMB systems. The Schroeder–Van Laar equation was employed for this purpose:

$$\ln x = \frac{\Delta H_A^f}{R}\left(\frac{1}{T_A^f} - \frac{1}{T^f}\right)$$

where x is the mole fraction of the more abundant component of a mixture whose melting terminates at T^f (in Kelvin); $\triangle H_A^f$ (cal mol^{-1}) and T_A^f (also in Kelvin) are the enthalpy of fusion and the melting point of the pure component A, respectively; and R is the gas constant, 1.9869 cal mol^{-1} K^{-1}.

In Figure 6, the calculated liquidus curves are traced versus composition in terms of independent components (TAA and AMB). According to the experimental data, the phase diagram can be conveniently divided into two temperature regions, on the basis of the temperature range

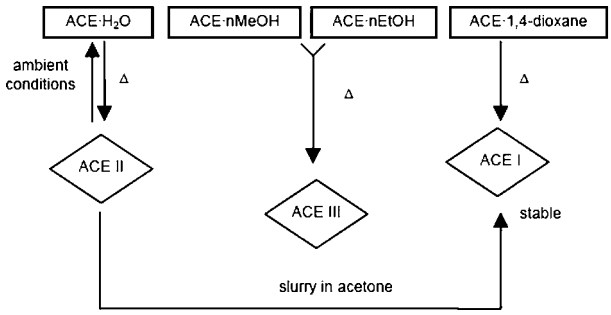

Figure 7. Scheme of relationships between ACE polymorphs and solvates (△ refers to the addition of heat).

relevant to the exothermal event (130–160°C) related to the reaction between TAA and AMB, leading to ACE.

In the lower region, TAA and AMB are present, while in the upper region TAA + ACE, ACE alone, or ACE + AMB can be found.

The superposition of data derived from DSC measurements on TAA–ACE, ACE–AMB, and TAA–AMB mixtures clearly indicates a satisfactory consistency only up to $x_{AMB} = 0.5$ with the theoretical model of a simple eutectic between TAA and ACE.

CONCLUSIONS

Six crystal forms of ACE (two polymorphs and four solvates) have been successfully isolated and identified. The existence of a third nonsolvated form, obtained from the alcoholates, can be hypothesized even though thus far its isolation at ambient condition could not be achieved. The thermodynamic and structural relationships between the various species are summarized in diagrammatic form in Figure 7.

The Schroeder–Van Laar equation proved to be a very useful tool for checking the consistency between the experimental data (DSC and HSM) and the theoretical model related to the general system showing complete miscibility in the liquid phase and complete immiscibility in the solid phase.

ACKNOWLEDGMENTS

EB, LRN, and MRC thank the University of Cape Town and the NRF (Pretoria) for research support.

MRC, FG, and RB also wish to acknowledge the financial support of the South Africa–Italy Programme on Research Co-operation, CHP Project No. 12, Solid-state properties of pharmaceutical compounds, Category: Medicine and Health.

REFERENCES

1. Grant DJW. 1998. Theory and origin of polymorphism. In: Brittain HG. editor. Polymorphism in pharmaceutical solids. New York: Marcel Dekker. pp 1–33.
2. Vippagunta SR, Brittain HG, Grant DJW. 2001. Crystalline solids. Adv Drug Del Rev 48:3–26.
3. Suyama H, Burioka N, Sako T, Kawasaki Y, Hitsuda Y, Shigeshiro K, Matsumoto Y. 1999. Pulmonary alveolar proteinosis treated with oral ambroxol hydrochloride and bronchoalveolar lavage. Yonago Acta Med 42:175–178.
4. Segura-Lozano F, Tenorio G. 1995. Treatment with ambroxol of the sicca keratoconjunctivitis associated with Sjögren syndrome. Rev Med Hosp Gen Mex 58:118–123.
5. Ferretti C, Coppi G, Blengio M, Genazzani E. 1992. Inhibitory effect of theophylline, theophylline-7-acetic acid, ambroxol and ambroxol-theophylline-7-acetate on rat lung cAMP phosphodiesterase isoenzymes. Int J Tissue React 14:31–36.
6. Zlatkov A, Peikov P, Danchev N, Ivanov D, Tsvetkova B. 1998. Synthesis, toxicological, pharmacological assessment, and in vitro bronchodilating activity of some 7-theophyllinylacetyloxyglycols. Arch Pharm 331:313–318.
7. Martinez Roldan C, Fernandez Brana M, Castellano B, Jose M. 1976. A theophylline acetate salt and its use in pharmaceutical compositions. GB 1438529 1976-06-09.
8. Cojocaru Z, Danila G, Nastase V. 1982. Theophylline-7-acetic acid N,N-diethylaminoethanol salt. RO 79918 B1982-09-30.
9. Kosmider S, Maslankiewicz A, Rohloff B. 1977. Salt of theophylline-7-acetic acid and xylocaine. PL 93084 1977-12-15.
10. Maslankiewicz A, Rohloff B. 1976. Salt of theophylline-7-acetic acid and procainamide. PL 83970 1976-05-20.
11. Szatmari I, Simon G, Vargay Z, Toth E, Szuts T. 1984. The fate of drotaverine-acephyllinate in rat and man. I. Absorption, distribution and excretion in the rat. Eur J Drug Metab Pharm 9:11–16.
12. Szentmiklosi P, Marton S. 1979. Practical importance of drug equivalence in preclinical research, with special emphasis on drotaverine and its salt with theophylline-7-acetic acid. Acta Pharm Hung 49:50–53.
13. Massaroli G. 1985. Ambroxol theophylline 7-acetate. Ger. Offen. 6 pp. DE 3425007 A1 1985-01-17.
14. Agliati G. 1996. Effects of a short course of treatment with acebrophylline on the mucus rheological characteristics and respiratory function parameters in patients suffering from chronic obstructive pulmonary disease. J Int Med Res 24:302–310.
15. Agliati G. 1995. Acebrophylline in the treatment of chronic obstructive pulmonary disease. Curr Ther Res Clin Exp 56:169–175.
16. Caira MR, Foppoli A, Sangalli ME, Zema L, Giordano F. 2004. Thermal and structural properties of ambroxol polymorphs. J Therm Anal Cal 77:653–662.
17. Giordano F, et al. unpublished results.
18. Giuseppetti G, Mazzi F, Tadini C, Giordano F, Bettinetti G, Sorrenti M, Gazzaniga A. 1998. Ambroxol theophylline-7-acetate monohydrate. Acta Crystallogr C C54:407–410.
19. Salas JM, Quirós M, Angustias Romero M, Sanchez M, Salas MA, Vilaplana R. 1995. Metal complexes of theophylline-7-acetic acid. Crystal structure of a nickel(II) compound containing non-coordinated theophylline-7-acetate ion. Polyhedron 14:611–616.
20. Burger A, Ramberger R. 1979. On the polymorphism of pharmaceuticals and other organic molecular crystals. I: Theory of thermodynamic rules. Mikrochim Acta 2:259–271.